Supporting Information

Single-crystal to single-crystal transition from a 7-fold interpenetrated coordination polymer to non-interpenetrated one by photochemical [2+2] polymerization and their sensing properties

Xiao-Yu Zhang, [a] Shu-Man Zhao, [a] Ran Li, [a, b] Zou-Hong Xu, [a] Min-Yan Wang, [a] Yu-Fei Jiang, [a] Kai Chen, [b] Yue Zhao*[a] and Wei-Yin Sun*[a]

a. *Coordination Chemistry Institute, State Key Laboratory of Coordination Chemistry, School of Chemistry and Chemical Engineering, Nanjing National Laboratory of Microstructures, Collaborative Innovation Center of Advanced Microstructures, Nanjing University, Nanjing 210023, China.*

b. *Collaborative Innovation Center of Atmospheric Environment and Equipment Technology, Jiangsu Key Laboratory of Atmospheric Environment Monitoring and Pollution Control, School of Environmental Science and Engineering, Nanjing University of Information Science & Technology, Nanjing 210044, China*

Email address: zhaoyue@nju.edu.cn (Y. Zhao)

Email address: sunwy@nju.edu.cn (W.Y. Sun)

X-ray crystallography

Single-crystal X-ray diffraction data were collected on a Bruker D8 Venture diffractometer with graphite-monochromated Ga Kα radiation (λ = 1.34139 Å). The integration of diffraction data and intensity corrections for the Lorentz and polarization effects were performed by using SAINT program.[1] Semi-empirical absorption corrections were applied using SADABS program.[2] The structures were solved by direct methods with SHELXT-2014, expanded by subsequent Fourier-difference synthesis, and all the non-hydrogen atoms were refined anisotropically on F^2 using the full-matrix least-squares technique using the SHELXL-2018 crystallographic software package.[3,4] The details of crystal parameters, data collection and refinements for **1** and **2** are listed in Table 1, and the selected bond lengths and angles are given in Table S1.

Table S1. Selected bond lengths (Å) and angles (°) for **1** and **2**.[a]

		1	
Zn(1)-O(1)#1	1.972(2)	O(1)-Zn(1)-N(2)#2	110.16(8)
Zn(1)-O(6)	1.9330(18)	O(6)-Zn(1)-O(1)#1	103.92 (9)
Zn(1)-N(1)	2.022(2)	O(6)-Zn(1)-N(1)	115.57 (8)
Zn(1)-N(2)#2	2.036(2)	O(6)-Zn(1)-N(2)	97.41 (8)
O(1)-Zn(1)-N(1) #1	106.90(8)	N(1)-Zn(1)-N(2)#2	121.49 (9)
		2	
Zn(1)-O(2)#1	1.940(4)	O(2)-Zn(1)-N(1)	111.83 (18)
Zn(1)-O(6)	1.935(4)	O(6)-Zn(1)-O(2)#1	104.46 (17)
Zn(1)-N(2)#2	2.059(4)	O(6)-Zn(1)-N(2)#2	114.27 (17)
Zn(1)-N(1)#2	2.041(5)	O(6)-Zn(1)-N(1)	117.77 (17)
O(2)-Zn(1)-N(2)#2	100.06 (17)	N(1)-Zn(1)-N(2)#2	107.06 (17)

[a]Symmetry transformations used to generate equivalent atoms: #1 -x+5/2, -y+1, z-1/2; #2 -x-1, y+1/2, -z+1/2 for **1**. #1 -x-3/2, -y+1, z-1/2; #2 -x+2, y-1/2, -z+1/2 for **2**.

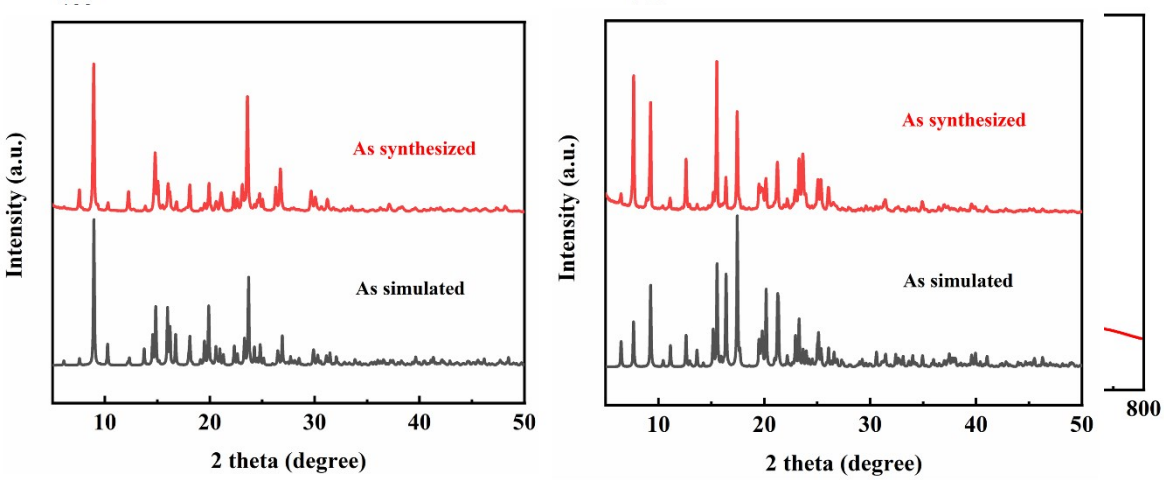

Fig. S1. (a) PXRD patterns of **1.** (b) PXRD patterns of **2.**

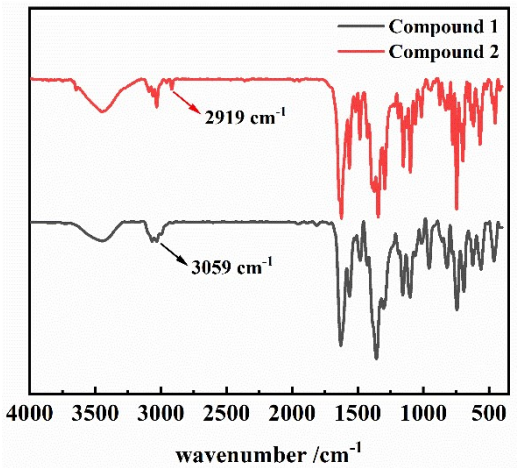

Fig. S3. FT-IR spectra of compound **1** and **2.**

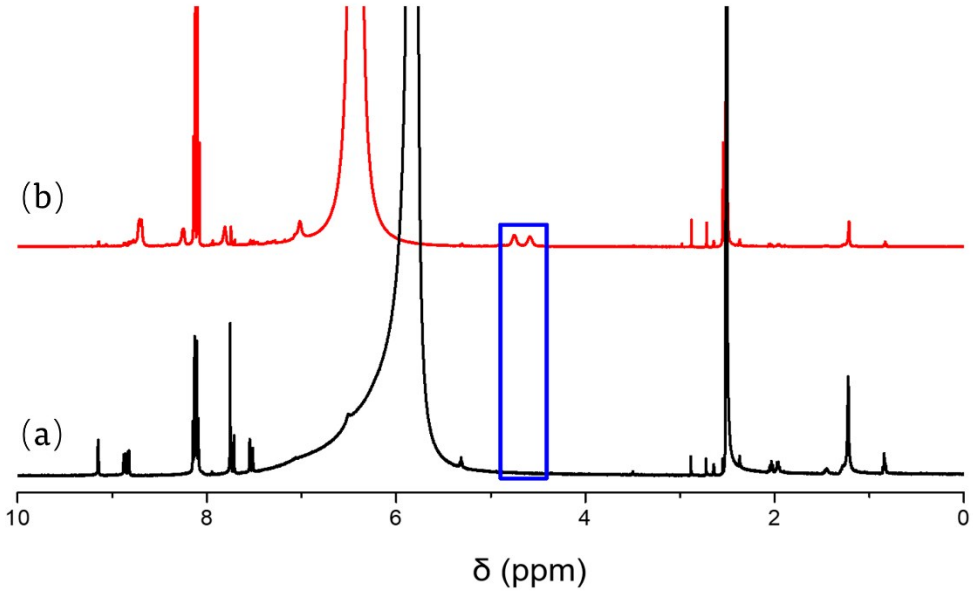

Fig. S4. The ^{1}HNMR results of **1** (a) and **2** (b) with a drop of HNO_3 in d^{6}-DMSO.

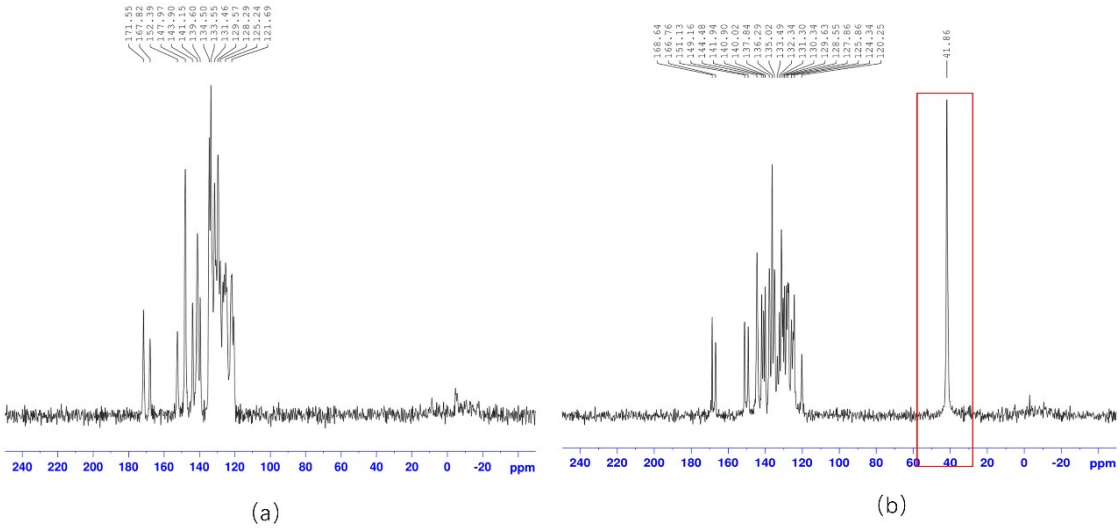

Fig. S5. The ^{13}C solid-state NMR results of **1** (a) and **2** (b).

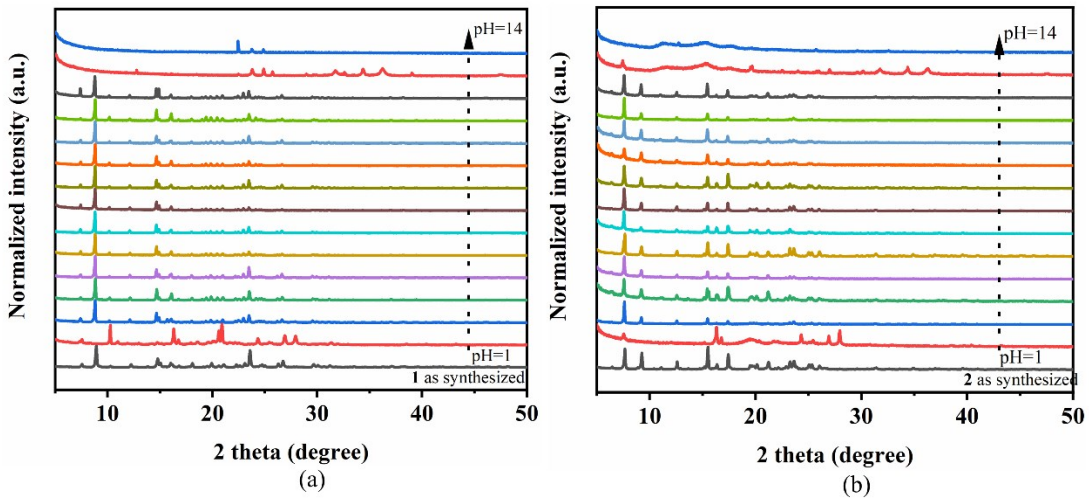

Fig. S6. The pH stability of **1** (a) and **2** (b).

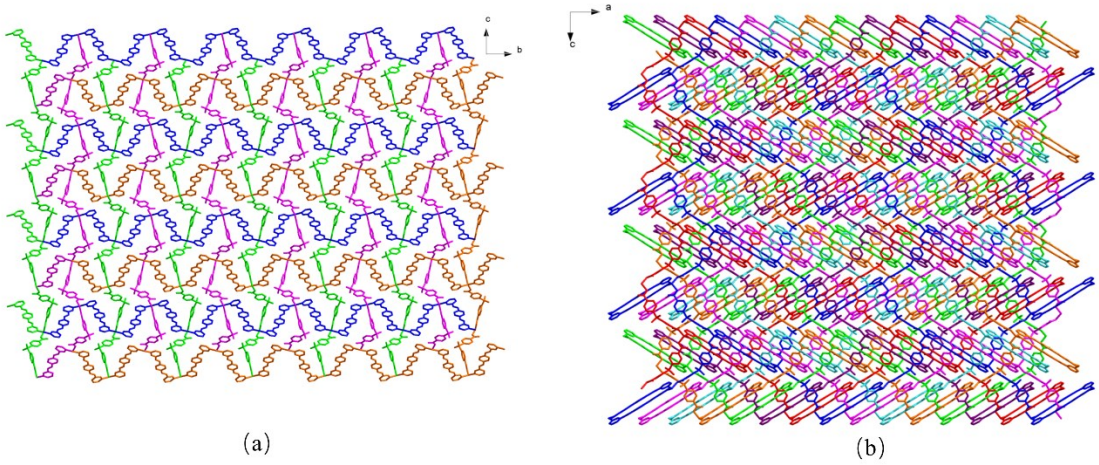

Fig. S7. The final 3D 7-fold interpenetrated frameworks of **1** along a-axis (a) and b-axis (b).

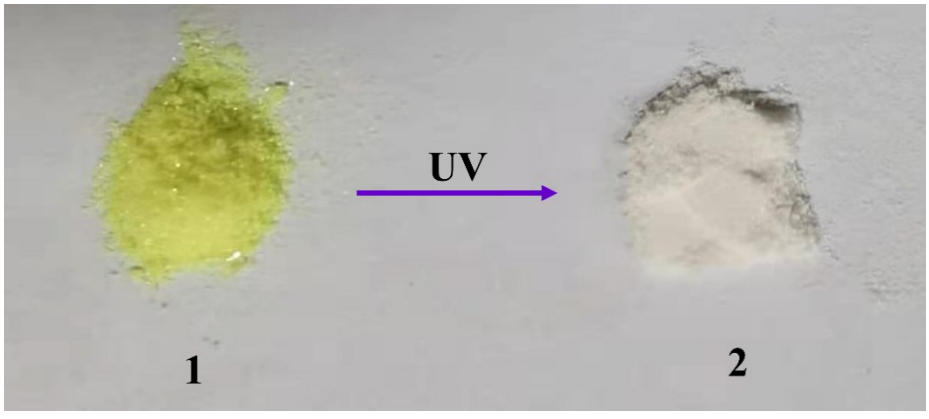

Fig. S8. The picture of Compound **1** and **2.**

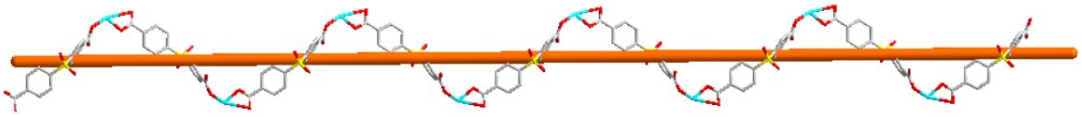

Fig. S9. The supramolecular helices in crystal structure of **1** and **2** composed of Zn (II) cation and sda^{2-}.

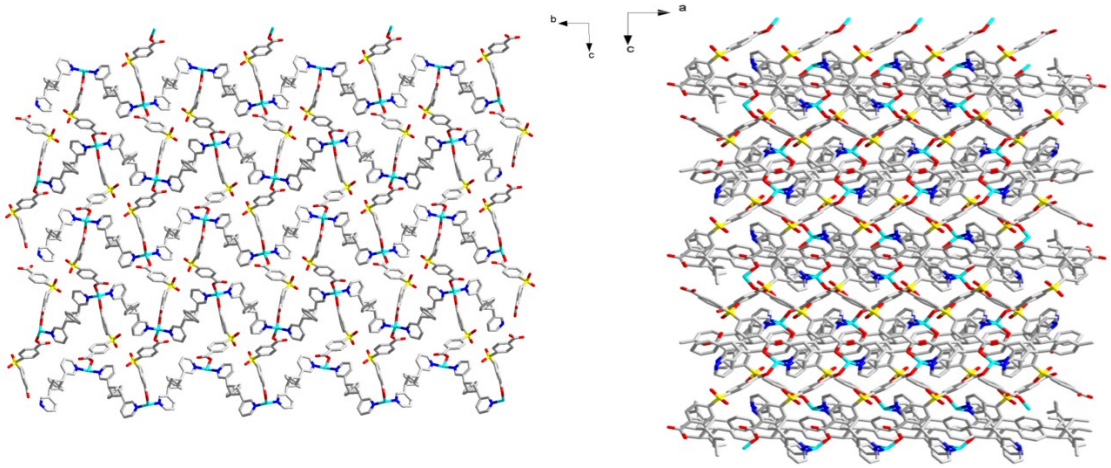

Fig. S10. The final 3D non-interpenetrated frameworks of **2** along with a-axis (a) and b-axis (b).

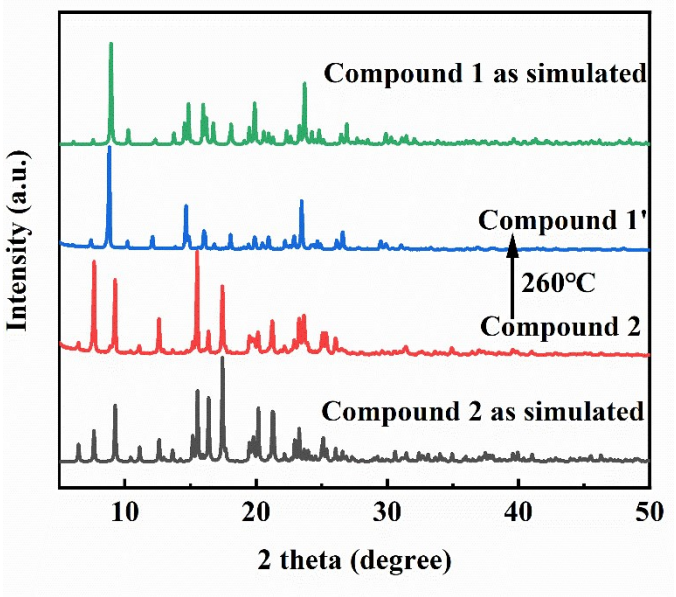

Fig. S11. Changes in the PXRD patterns of compound **2** upon heated at 260 ℃.

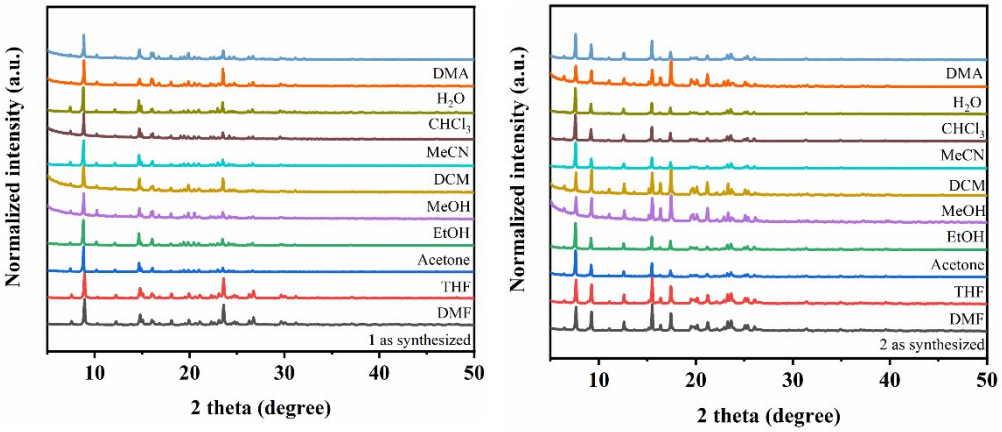

Fig. S12. The stability of **1**(a) and **2**(b) in different solvents.

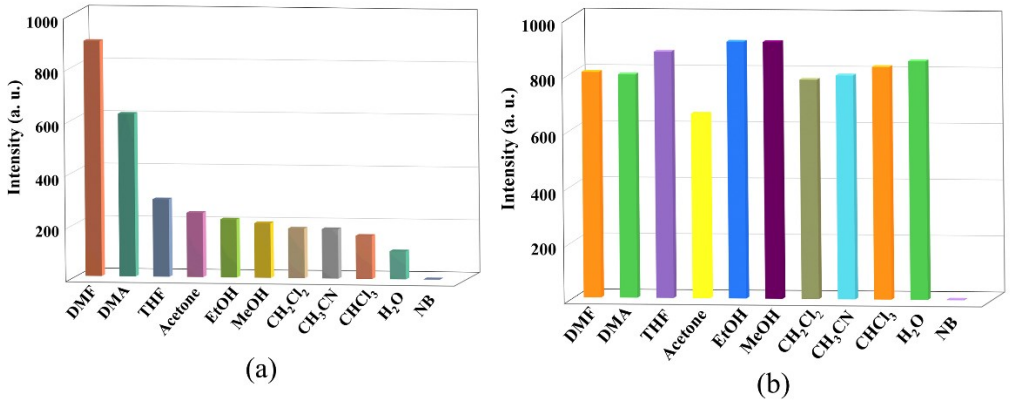

Fig. S13. The fluorescence intensity of **1**(a) and **2**(b) in different solvents.

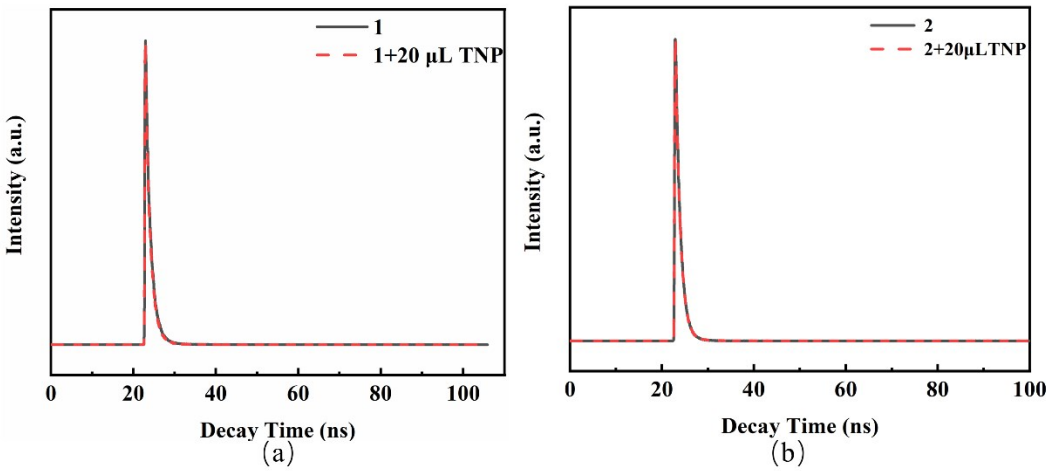

Fig. S14. Lifetimes of **1** (a) and **2** (b) dispersed in DMF before and after the addition of TNP.

Table S2. Standard deviation and detection limit calculation for TNP.

	1	**2**
1	823.758577	822.049487
2	823.463198	821.939862
3	824.041157	822.175866
4	823.7543107	822.055072
Standard deviation(σ)	0.0964291	0.0964291
Slope (m)	$3.5 \times 10^4 M^{-1}$	$4.1 \times 10^4 M^{-1}$
Detection limit (3σ/m)	$2.0 \times 10^{-5} M$	$7.0 \times 10^{-6} M$

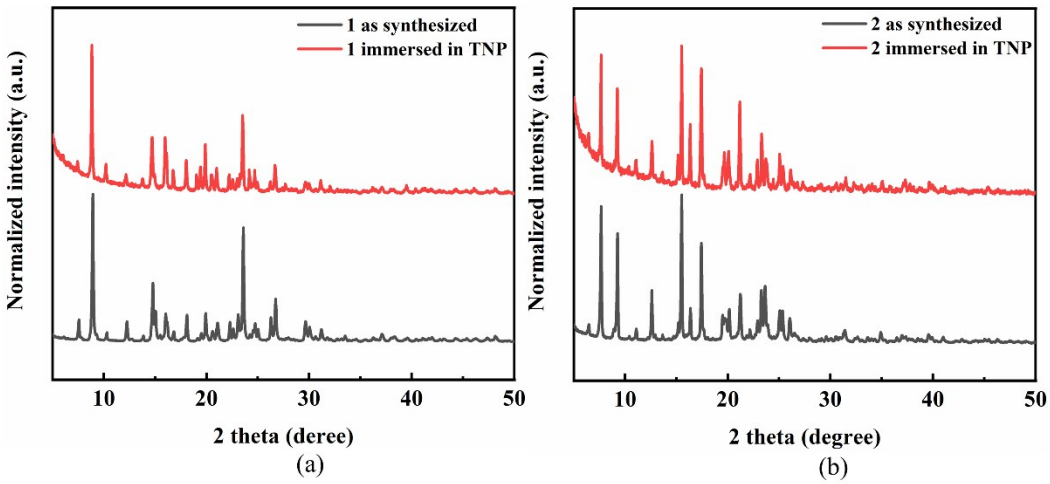

Fig. S15. PXRD patterns of **1** (a) and **2** (b) before and after soaking in the solution of TNP.

References

1 SAINT, *Program for Data Extraction and Reduction*, Bruker AXS, Inc., Madison, WI, 2001.

2 G. M. Sheldrick, *SADABS*, *Program for Empirical Adsorption Correction of Area Detector Data*. University of Gottingen, Gottingen, Germany, 2003.

3 G. M. Sheldrick, *SHELXS-2018, Program for the Crystal Structure Solution*, University of Gottingen, Gottingen, Germany, 2018.

4 G. M. Sheldrick, *SHELXL-2018, Program for the Crystal Structure Solution*, University of Gottingen, Gottingen, Germany, 2018.